



Journal of Geophysical Research: Space Physics

RESEARCH ARTICLE

10.1002/2017JA024785

Key Points:

- A new formalism is presented for gravity wave damping by ion friction for arbitrary propagation and geomagnetic field geometry
- For harmonics propagating meridionally, ion friction maximizes over the magnetic poles and decays to zero over the equator
- Estimated the influence of anisotropy of ion damping on gravity wave drag, induced cooling/heating rates, and temperature variance

Correspondence to:

A. S. Medvedev, medvedev@mps.mpg.de

Citation:

Medvedev, A. S., Yigit, E., & Hartogh, P. (2017). Ion friction and quantification of the geomagnetic influence on gravity wave propagation and dissipation in the thermosphere-ionosphere. *Journal of Geophysical Research: Space Physics*, 122. https://doi.org/10.1002/2017JA024785

Received 14 SEP 2017 Accepted 15 NOV 2017 Accepted article online 20 NOV 2017

Ion Friction and Quantification of the Geomagnetic Influence on Gravity Wave Propagation and Dissipation in the Thermosphere-Ionosphere

Alexander S. Medvedev¹, Erdal Yiğit², and Paul Hartogh¹

¹ Max Planck Institute for Solar System Research, Göttingen, Germany, ² Department of Physics and Astronomy, George Mason University, Fairfax, VA, USA

Abstract Motions of neutrals and ions in the thermosphere-ionosphere (TI) do not, generally, coincide due to the presence of the geomagnetic field and associated electromagnetic forces affecting plasma. Collisions of ions with gravity wave (GW)-induced motions of neutrals impose damping on the latter. We derive a practical formula for the vertical damping rate of GW harmonics that accounts for the geometry of the geomagnetic field and the direction of GW propagation. The formula can be used in parameterizations of GW effects developed for general circulation models extending from the lower atmosphere into the mesosphere and thermosphere. Vertical damping of GW harmonics by ion-neutral interactions in the TI depends on the geometry of the geomagnetic field but not the strength of the latter. The ion damping of harmonics propagating in the meridional direction (in the geomagnetic coordinates) maximizes over the poles and reduces to zero over the equator. Waves propagating in the zonal direction are uniformly affected by ions at all latitudes. Accounting for the anisotropy produces changes in the GW drag in the *F* region of more than 100 m s⁻¹ d⁻¹, cooling/heating rates of more than 15 K d⁻¹, and in GW temperature variance of disturbances by more than 5 K.

1. Introduction

It has been long known that the thermosphere is routinely disturbed by gravity waves (GWs) propagating from below. In some cases, the sources of strong wave activity in the thermosphere-ionosphere can be traced back to various phenomena in the troposphere, like severe storms (Hung et al., 1979), tsunami (Artru et al., 2005; Garcia et al., 2014; Hickey, 2011), deep convection (Miller et al., 2015), or flow over mountains (de la Torre et al., 2014). Modeling studies have demonstrated that GWs of various scales excited in the troposphere can effectively propagate to the upper thermosphere surviving filtering in the middle atmosphere and damping by exponentially growing with height molecular diffusion and thermal conduction (e.g., Fritts & Lund, 2011; Gavrilov & Kshevetskii, 2013; Heale et al., 2014; Yiğit et al., 2009). There are indications that GWs from sources in the troposphere can also excite secondary waves that can reach the thermosphere-ionosphere (TI) region (Vadas & Crowley, 2010). Over the last decade, investigations have revealed that these waves not only create high-altitude signatures of various processes occurring in the lower atmosphere but greatly contribute to the momentum and energy budget of the middle and upper thermosphere, similar to their effects in the middle atmosphere (e.g., see Yiğit & Medvedey, 2015 for a review). They affect the zonal mean thermospheric circulation (Miyoshi et al., 2014; Yiğit et al., 2009, 2012), temperature (Yiğit & Medvedev, 2009), thermal tides (Yiğit & Medvedev, 2017), alter thermospheric variability (Forbes et al., 2016; Yiğit et al., 2014) and play a significant role during sudden stratospheric warmings (Goncharenko et al., 2013; Liu et al., 2013; Yiğit & Medvedev, 2012; 2016). Obviously, the influence of small-scale GWs of tropospheric origin must be taken into account, if one wants to understand the energy and momentum budget of the thermosphere and better reproduce its dynamics.

The upper atmosphere is a partially ionized fluid comprising the neutral thermosphere and the ionosphere, which is the ionized component. The primary interactions between neutrals and ions occur through collisions. If there were no geomagnetic field, motions of ions would be driven by the much more abundant neutrals, and their dynamical response to GW disturbances in the thermosphere-ionosphere (TI) would be very similar to that of other atmospheric trace gases. In the presence of Earth's intrinsic magnetic field, GW-induced motions of the ionized component are affected by electromagnetic forces and may, generally, not coincide with that

©2017. American Geophysical Union. All Rights Reserved.



of neutrals. This mismatch gives rise to an additional force—ion drag—that neutral motions associated with GWs experience in the thermosphere. There is a multitude of magnetohydrodynamic (MHD) phenomena associated with a passage of GWs in the TI. In this paper, we focus on dissipative effects caused by ion drag on GWs. This dissipation due to ion friction controls attenuation of small-scale waves during their vertical propagation, determines how high GW harmonics penetrate into the TI, and defines the rate, at which they supply momentum and energy to the larger-scale flow.

Studies of GW propagation in the ionosphere started already in the 1950s. In part, they were motivated by the discovery of traveling ionospheric disturbances (TIDs) (Munro, 1950), which have been identified as a manifestation of GW-induced disturbances of neutral winds. TIDs are routinely observed in the ionosphere, especially by incoherent scatter radars, and their relationship to GWs have been studied by a number of authors (e.g., Hocke & Schlegel, 1996; Kirchengast, 1997). The main theoretical results concerning the influence of ion drag on acoustic-gravity waves have been obtained in the works of Hines (1955), Liu and Yeh (1969), and Hines and Hooke (1970), and further extended in the papers of Francis (1973), Hickey and Cole (1987), Miesen et al. (1989), and Miesen (1991). They derived dispersion relations of various complexities for acoustic-gravity waves in the presence of ion drag and magnetic field. Some of these works analytically explored peculiarities of GW propagation affected by ion friction. Understandably, the analytical calculations were tractable only under very idealized conditions and the derived formulas were cumbersome. Therefore, these works only demonstrated some characteristics of GW propagation in certain directions. Klostermeyer (1972) attempted numerical simulations with a linearized wave model under more realistic conditions, thus allowing for comparison with observations deduced from ionograms.

The increasing interest in the influence of ion friction on GWs is associated with the need for accounting for dissipative effects in GW parameterizations in order to gain a more precise description of wave propagation in the whole atmosphere system. Essentially, wave obliteration is a major physical process through which waves impact the mean flow. Present-day general circulation models (GCMs) extending to the thermosphere still do not sufficiently resolve small-scale GWs, despite the tendency to increase grid resolutions. Therefore, effects of subgrid-scale waves have to be parameterized in models. Any physically based GW scheme must quantify vertical damping rates, including those due to ion friction. To the best of our knowledge, the only parameterization employed in "whole atmosphere" GCMs that accounts for ion drag is the nonlinear spectral scheme developed in the work by Yiğit et al. (2008) (see the paper of Yiğit and Medvedev, 2017, for the most recent application in the Coupled Middle Atmosphere Thermosphere-2 GCM). Sometimes, this scheme is referred to as the whole atmosphere GW parameterization in analogy with whole atmosphere GCMs. There, attenuation of GW harmonics by ion-neutral collisions was treated in a simplified form that neglected the shape of the magnetic field as well as the geometry of wave propagation (Yiğit et al., 2008, section 3.4). The purpose of this study is to derive a general but practical representation of geomagnetic influence on GWs suitable for use in GW parameterizations.

This paper is structured as follows: In section 2, we review the physics of ion-neutral coupling and introduce the basis for further parameterization of GW dissipative effects in the ionosphere. The mathematical development leading to the parameterization of the vertical damping rate due to interactions with ions is described in section 3 and discussed in a broader context in section 4. Section 5 outlines the whole atmosphere GW parameterization and its settings. Results of the calculations are given in section 6. Conclusions are summarized in section 7.

2. Interaction of lons and Neutrals in Gravity Wave Motions

In general, the momentum balance for a particle of species "s" with the mass density ρ_s moving with the three-dimensional velocity \mathbf{v}_s can be represented in a compact form by (Yiğit, 2017, Equation 5.10)

$$\frac{d\mathbf{v}_{s}}{dt} = -\frac{1}{\rho_{s}} \nabla p_{s} + \mathbf{g} + \mathbf{F} - \sum_{j} v_{sj} (\mathbf{v}_{s} - \mathbf{v}_{j}), \tag{1}$$

where the first two terms on the right-hand side are the pressure and gravitational forces, respectively. **F** encapsulates all other nonelectromagnetic forces (per unit mass) that include, in particular, diffusion and Coriolis force $2\rho \mathbf{v}_s \times \Omega$, Ω being the planetary angular rotation frequency. The material derivative of the wind velocity $\mathbf{dv}_s/dt = \partial \mathbf{v}_s/\partial t + (\mathbf{v}_s \cdot \nabla)\mathbf{v}_s$ may also include nonlinear terms that arise due to planet's curvature, when written in spherical coordinates. The last term in (1) accounts for the momentum transfer to the particle species "s" due to collisions with all other particle species denoted by "j".



Following the above generalization, the starting point of our consideration is the momentum equation for a neutral gas in the presence of collisions with ions and electrons

$$\rho \frac{d\mathbf{v}}{dt} = -\nabla p - \rho \mathbf{g} + \rho \mathbf{F} - \rho_i v_{\text{in}} (\mathbf{v} - \mathbf{v}_i) - \rho_e v_{\text{en}} (\mathbf{v} - \mathbf{v}_e), \tag{2}$$

where the indices i and e denote variables for ions and electrons, correspondingly; neutral variables are written without indices; ρ , p, and $\mathbf{v} = (u, v, w)$ are the neutral mass density, pressure, and the wind velocity, respectively; $\mathbf{g} = (0, 0, -g)$ is the acceleration of gravity. In the context of neutrals dynamics, the last two terms in the right-hand side of (2) describe ion-neutral and electron-neutral momentum exchanges, respectively, where $v_{\rm in}$ and $v_{\rm en}$ are the effective collisional frequencies of ions and electrons with neutral particles, respectively. Conservation of momentum requires that $\rho_i v_{\rm in} = \rho v_{\rm ni}$ and $\rho_e v_{\rm en} = \rho v_{\rm ne}$, where $v_{\rm ni}$ and $v_{\rm ne}$ are the effective collisional frequencies of neutrals with ions and electrons, respectively. Note that these pairs of frequencies can be used alternatively, but, in general, they are not symmetric quantities, that is, $v_{ii} \neq v_{ii}$.

If \mathbf{v}_i and \mathbf{v}_e are known, equation (2), complemented by the continuity and thermodynamic equations, will represent a closed set for neutral field variables. Without electromagnetic forces, collisions would rapidly equalize velocities ($\mathbf{v}_i = \mathbf{v}_e = \mathbf{v}$), and motions of charged components would not differ from those of neutrals, as in the case with passive atmospheric trace gases. In the presence of the geomagnetic field, this is no longer the case. Hence, one has to explicitly consider momentum equations for ions and electrons. The latter can be simplified, because ion and electron pressure, buoyancy, and Coriolis forces are much weaker than the Lorentz force, and their time derivatives can be neglected for phenomena with spatial scales longer than some tens of meters and frequencies below the radio range, yielding the following relations for the electron and ion momentum balances (e.g., Vasyliūnas, 2012, section 3.2):

$$0 = -\rho_i v_{in}(\mathbf{v}_i - \mathbf{v}) - \rho_i v_{ie}(\mathbf{v}_i - \mathbf{v}_e) + e n_i (\mathbf{E} + \mathbf{v}_i \times \mathbf{B}), \tag{3}$$

$$0 = -\rho_e v_{en}(\mathbf{v}_e - \mathbf{v}) - \rho_e v_{ej}(\mathbf{v}_e - \mathbf{v}_j) - en_e(\mathbf{E} + \mathbf{v}_e \times \mathbf{B}). \tag{4}$$

In (3) and (4), it is assumed that the ions are single charged, that is, $e_i = -e_e = e$, where -e is the charge of an electron; n_e and n_i are number density of electrons and ions, correspondingly; **E** and **B** are the electrical and magnetic (induction) field strengths, respectively.

Combining equations (2), (3), and (4) yields

$$\rho \frac{d\mathbf{v}}{dt} = -\nabla \rho + \rho \mathbf{F} + \rho' \mathbf{E} + \mathbf{J} \times \mathbf{B},\tag{5}$$

where $\mathbf{J}=e(n_i\mathbf{v}_i-n_e\mathbf{v}_e)$ is the microscopic current density and $\rho'=e(n_i-n_e)=0$ under the assumption of quasi-neutrality $(n_i=n_e=n)$ of ionospheric plasma. Note that the terms describing mutual drag between any pair of particles in (2)–(4) must be equal in magnitude and have opposite signs due to conservation of momentum. Then, after summation, these internal friction forces cancel each other, because the momentum exchanges between parts of the system do not change the total momentum of the system. Equation (5) represents an alternative to (2) formulation, in which the "ion" drag due to the relative drift of neutrals and charged particles is replaced with the Ampère's force $\mathbf{J} \times \mathbf{B}$ associated with the electric current due to the mismatch of ion and electron velocities $\mathbf{v}_i - \mathbf{v}_e \neq 0$.

The generalized Ohm's law relates the current density **J** with the electric field **E** that includes also the portion induced by a motion of charged particles in the magnetic field **B**.

$$\mathbf{J} = \sigma_{\parallel} \mathbf{E}_{\parallel} + \sigma_{p} (\mathbf{E} + \mathbf{v} \times \mathbf{B})_{\perp} + \frac{\sigma_{H}}{R} \mathbf{B} \times (\mathbf{E} + \mathbf{v} \times \mathbf{B})_{\perp}, \tag{6}$$

where σ_{\parallel} , σ_p , and σ_H are the parallel, perpendicular (Pedersen), and Hall conductivities, respectively; \mathbf{E}_{\parallel} and \mathbf{E}_{\perp} are the components parallel and perpendicular to \mathbf{B} , correspondingly; $\mathbf{v} \times \mathbf{B}$ accounts for the induced dynamo field owing to the relative motion of the neutrals; $B = (\mathbf{B} \cdot \mathbf{B})^{1/2}$ is the magnitude of the vector \mathbf{B} . The term with σ_{\parallel} vanishes, when (6) is substituted into (5), because E_{\parallel} does not contribute to $\mathbf{J} \times \mathbf{B}$. For analyzing contributions of the other terms, we consider the expressions for σ_p and σ_H (e.g., Yiğit, 2017, equations (3.55) and (3.56))

$$\sigma_p = e^2 n_i \left[\frac{v_e}{m_e \left(\omega_{ge}^2 + v_e^2 \right)} + \frac{v_{in}}{m_i \left(\omega_{gi}^2 + v_{in}^2 \right)} \right], \tag{7}$$



$$\sigma_{H} = e^{2} n_{i} \left[\frac{\omega_{ge}}{m_{e} \left(\omega_{ge}^{2} + v_{e}^{2} \right)} - \frac{\omega_{gi}}{m_{i} \left(\omega_{gi}^{2} + v_{in}^{2} \right)} \right], \tag{8}$$

where $\omega_{\rm ge}=eB/m_e$ and $\omega_{\rm gi}=eB/m_i$ are gyrofrequencies (or cyclotron frequencies) of electrons and ions, whose masses are m_e and m_i , correspondingly; and $v_e=v_{\rm ei}+v_{\rm en}$ represents total collision frequencies experienced by electrons due to the presence of ions and neutrals. In the F region, the ions and electrons are magnetized; that is, the gyrofrequencies greatly exceed the corresponding collisional frequencies: $\omega_{\rm gi}\gg v_{\rm in}$ (~300 s⁻¹ versus ~10 s⁻¹), and $\omega_{\rm qe}\gg v_e$ (~10⁷ s⁻¹ versus ~10³ s⁻¹). This simplifies (7) and (8) to

$$\sigma_{\rho} \approx \frac{\rho_{i} \nu_{\rm in}}{B^{2}} = \frac{\rho \nu_{\rm ni}}{B^{2}},\tag{9}$$

and

$$\sigma_H = 0$$
.

More precisely, $\sigma_p \gg \sigma_H$ above \sim 120 km. Below this height, σ_H exceeds σ_p (e.g., Kelley, 2009, Figures B.2 – B.6).

Because our focus is on waves, all the hydrodynamic equations must be linearized around an appropriately defined mean. The electromagnetic variables in (5) and (6) must also be split into the mean and deviations. For Earth, a good approximation for the mean is $\vec{\bf E}=0$ and $\vec{\bf B}={\bf B}_0$, where bars denote the mean, and ${f B}_0$ is the undisturbed geomagnetic field. To close the set of equations for deviations describing the MHD system, accordingly linearized Maxwell's equations must be added. Such system will describe additional magnetogravity wave modes, and the corresponding dispersion equation will have higher order in frequency. For further understanding processes in the TI described by this system, it is instructive to consider the physical causation. In the absence of GWs, ions and electrons gyrate around the magnetic field lines producing no macroscopic electric current. When a GW disturbance v' arrives from below, it induces the electric current $\mathbf{J}' = \mathbf{v}' \times \mathbf{B}_0$, which is created by the charged particles drifting along the magnetic lines (while continuing their gyration). Disturbances J' trigger GW-induced variations of E' and B' that, in turn, feed back to the hydrodynamic GWs via the Ampère force. This consideration can be simplified, if only the geomagnetic influence on the GW propagation is of primary interest. Hines (1955), Miesen et al. (1989), and Miesen (1991) reported that, for typical ionospheric conductivities, the electromagnetic and hydrodynamic parts are weakly coupled in the sense that the induced variations of the electromagnetic field weakly affect the hydrodynamic variables. Therefore, terms containing \mathbf{E}' and \mathbf{B}' can be neglected, and only the dynamo-part term $\mathbf{v}' \times \mathbf{B}_0 \times \mathbf{B}_0$ is retained in (5). Of course, if generation of electromagnetic disturbances by GWs is of interest, the Maxwell equations cannot be decoupled (e.g., Pogoreltsev, 1996). Thus, together with (9) and neglected σ_H , the right-hand side of the linearized equation (5) describing the geomagnetic influence on GWs takes the form

$$\mathbf{J} \times \mathbf{B} \approx \sigma_{n} \mathbf{v}' \times \mathbf{B}_{0} \times \mathbf{B}_{0} = -\rho v_{n} \left[\mathbf{v}' - (\mathbf{v}' \cdot \mathbf{b}) \mathbf{b} \right], \tag{10}$$

where $\mathbf{b} = \mathbf{B}_0/B$ is the unit vector in the direction of the magnetic field. See also (A2) in Appendix A.

It is immediately seen from (10) that, in the first approximation, the ionospheric feedback on GWs depends only on the geometry of the magnetic field but not on the field strength. Further physical understanding can be gained from comparison of (10) with the collisional terms in the right-hand part of (2). These two terms coincide if collisions with electrons are neglected in (2) compared to those with ions, and the ion velocity is induced by (and equal to) the projection of GW wind oscillations \mathbf{v}' on the direction of the magnetic field. Note also that (10) represents a compact form of the term considered by Liu and Yeh (1969). Unlike in the latter paper, where the solution was obtained for only harmonics propagating in two specific directions, our goal is to develop a practical parameterization that can be applied to all directions and used with all GW schemes. We pursue this task in the next section.

3. Parameterization of Vertical Damping Rates

We first introduce certain physically suitable simplifications. One assumption deals with the shape of the geomagnetic field, which can be closely approximated by a dipole in the F region ionosphere. In the geomagnetic coordinates, which are used in this section, this means that $\mathbf{b} = (0, b_y, b_z)$. If γ is the angle between the local vertical and the unit vector \mathbf{b} , then the components $b_v = \sin \gamma$ and $b_z = \cos \gamma$ can be substituted into (10).



Next, we adopt the hydrostatic approximation $(\partial p/\partial z = -\rho g)$, thus filtering out acoustic waves. Also, we consider only midfrequency GW harmonics with frequencies much greater than the local Coriolis frequency, but much smaller than the buoyancy frequency: $f \ll \tilde{\omega} \ll N$. These assumptions are typical for GW parameterizations that are currently in use (e.g., Fritts & Alexander, 2003; Medvedev & Klaassen, 1995, 2000; Yiğit et al., 2008). Thus, the momentum equation (5) supplemented by the thermodynamic and continuity equations represents a closed set of equations governing the GW dynamics (hereafter, primes are dropped for disturbances, unless otherwise explicitly stated)

$$\frac{\mathrm{d}u}{\mathrm{d}t} + \frac{1}{\rho_0} \frac{\partial p}{\partial x} + \nu_{\mathrm{ni}} u = 0, \tag{11}$$

$$\frac{\mathrm{d}v}{\mathrm{d}t} + \frac{1}{\rho_0} \frac{\partial p}{\partial y} + \nu_{\mathrm{ni}}(v \cos^2 \gamma - w \cos \gamma \sin \gamma) = 0, \tag{12}$$

$$\frac{\partial p}{\partial z} + \rho g + \rho_0 v_{\text{ni}}(w \sin^2 \gamma - v \cos \gamma \sin \gamma) = 0, \tag{13}$$

$$\frac{\mathrm{d}\rho}{\mathrm{d}t} + w\frac{\partial\rho_0}{\partial z} = 0,\tag{14}$$

$$\frac{\partial u}{\partial x} + \frac{\partial v}{\partial y} + \frac{1}{\rho_0} \frac{\partial \rho_0 w}{\partial z} = 0. \tag{15}$$

Note the form of the continuity equation (15), which differs from the usual one under the anelastic approximation, but coincides with the equation in (log)-pressure coordinates. Equation (15) is consistent with the midfrequency approximation, simplifies the derivation, and does not affect the sought after result—the expression for the damping rate by ion friction. In the above equations, $\rho_0 = \rho_0(z)$ is the background-neutral density. Density disturbances ρ can be eliminated by applying d/dt to (13) and substituting the result into (14):

$$\frac{\mathrm{d}}{\mathrm{d}t}\frac{\partial p}{\partial z} - gw\frac{d\rho_0}{dz} + \rho_0 v_{\mathrm{ni}}\frac{\mathrm{d}}{\mathrm{d}t}(w\sin^2\gamma - v\cos\gamma\sin\gamma) = 0. \tag{16}$$

Equations (11), (12), (15), and (16) represent a set for u,v,w, and p. Assuming that wave disturbances are composed of plane wave harmonics $\sim \exp\left[i(k_xx+k_yy+mz-\omega t)\right]$, where ω is the frequency and (k_x,k_y,m) are the horizontal and vertical components of the wave vector \mathbf{k} , we find a dispersion relation for GWs affected by the magnetic field by equating the determinant of the matrix to zero

$$\det\begin{pmatrix} -i\tilde{\omega} + v_{n_{1}} & 0 & 0 & i\rho_{0}^{-1}k_{x} \\ 0 & -i\tilde{\omega} + v_{n_{1}}\cos^{2}\gamma & -v_{n_{1}}\cos\gamma\sin\gamma & i\rho_{0}^{-1}k_{y} \\ 0 & iv_{n_{1}}\tilde{\omega}\cos\gamma\sin\gamma & N^{2} - iv_{n_{1}}\tilde{\omega}\sin^{2}\gamma & m\tilde{\omega}\rho_{0}^{-1} \\ ik_{x} & ik_{y} & im - H^{-1} & 0 \end{pmatrix} = 0.$$
 (17)

In (17), $\tilde{\omega} = \omega - k_x \bar{u} - k_y \bar{v}$ is the intrinsic frequency, $H^{-1} = -[\rho_0^{-1} \mathrm{d} \rho_0/\mathrm{d} z]^{-1}$ is the scale height and $N^2 = -(g/\rho_0)(\mathrm{d}\rho_0/\mathrm{d}z)$ is the square of the Brunt-Väisälä frequency under the Boussinesq approximation. The dispersion relation (17) has to be solved for the complex vertical wave number $m = m_r + i m_i$, where the imaginary part m_i would give the sought after vertical damping rate. The analytical solution of (17) is cumbersome. Instead, we note that $v_{\mathrm{ni}} \ll \tilde{\omega}$ at F region heights (except in the vicinity of critical levels $\tilde{\omega} \to 0$). This allows for introducing a small parameter $\varepsilon = v_{\mathrm{ni}}/\tilde{\omega}$. Because the determinant is equal to zero, all terms in a row or column of the matrix can be multiplied or divided by the same nonzero quantity. Performing such algebra with rows and columns of (17), we transform the latter to a more compact form:

$$\begin{vmatrix}
-1 - i\varepsilon & 0 & 0 & k_x \\
0 & -1 - i\varepsilon \cos^2 \gamma & i\varepsilon \cos \gamma \sin \gamma & k_y \\
0 & -i\varepsilon \cos \gamma \sin \gamma & \frac{N^2}{\hat{\omega}^2} - i\varepsilon \sin^2 \gamma & m \\
k_x & k_y & m + \frac{i}{\mu} & 0
\end{vmatrix} = 0.$$
(18)

If $\varepsilon = 0$ and there was no term containing the scale height H, the matrix (18) would be pure real and symmetric. More generally, it would be Hermitian, that is, whose real part is symmetric and the imaginary part is



antisymmetric. Hermitian matrices describe conservatively propagating waves, while effects of growth and/or attenuation are associated with non-Hermitian parts. In the case at hand, the non-Hermitian term containing H describes wave amplitude growth with height due to density stratification. If $\varepsilon \neq 0$, the geomagnetic effects contribute to the Hermitian part (antisymmetric nondiagonal terms) and to the non-Hermitian one (the diagonal imaginary terms). Thus, one can expect from the mathematical form of the matrix (18) that the geomagnetic effects modify the conservative propagation as well as introduce dissipation.

We proceed with the mathematical development further and calculate the determinant (18) retaining only the terms not higher than $O(\varepsilon)$:

$$-i\frac{N^2k_h^2}{\tilde{\omega}^2} + \left(im^2 - \frac{m}{H}\right) + \varepsilon \left[-\left(m^2 + \frac{im}{H}\right)(1 + \cos^2\gamma) - k_h^2\sin^2\gamma - \frac{ik_y\cos\gamma\sin\gamma}{H} + \left(k_x^2\cos^2\gamma + k_y^2\right) \right] = 0,$$
(19)

where $k_h^2 = k_x^2 + k_y^2$ denotes the squared total horizontal wave number. Equation (19) encapsulates a set of the quadratic with respect to the vertical wave number equations for real and imaginary parts. Relying on the smallness of ε , one can seek the solution of (19) in the asymptotic form by assuming $m = m_0 + \varepsilon m_1 + \varepsilon^2 m_2 + ...$, where $m_0 = m_{0r} + i m_{0i}$, $m_1 = m_{1r} + i m_{1i}$, etc. Substituting the above expansion into (19) and equating to zero separately the real and imaginary parts, we obtain in the zeroth order $O(\varepsilon^0)$ (essentially, from the first line of (19) the familiar solution for GWs:

$$m_{0i} = -\frac{1}{2H},\tag{20}$$

$$m_{0_{\rm f}}^2 = \frac{N^2 k_h^2}{\tilde{\omega}^2} - \frac{1}{4H^2}. (21)$$

Equation (20) accounts for the exponential growth of wave amplitudes with height due to density stratification, while (21) represents the dispersion relation for GWs propagating without dissipation.

In the first order in ε , the solution of (19) is

$$m_{1r} = \frac{k_y}{2m_{0r}H}\cos\gamma\sin\gamma,\tag{22}$$

$$m_{1i} = \frac{1}{2m_{0r}} \frac{N^2}{\tilde{\omega}^2} \left(k_x^2 + k_y^2 \cos^2 \gamma \right) + \frac{k_h^2 \sin^2 \gamma}{2m_{0r}}.$$
 (23)

It is seen that geomagnetic effects alter propagation characteristics of GWs in the first order of ε (22) and introduce a vertical damping with the rate m_{1j} . Most of GW parameterizations, including those of Yiğit et al. (2008) and its predecessor for middle atmosphere GCMs (Medvedev & Klaassen, 1995, 2000), consider only short vertical-scale harmonics with $m_r H \gg 1$. For such harmonics, the correction (22) to the dispersion relation can be neglected. Similarly, the zeroth order in ε (undisturbed) dispersion relation (21) simplifies to

$$m_{0r}^2 = \frac{N^2 k_h^2}{\tilde{\omega}^2}. (24)$$

Next, we explore the ratio between the second and first terms in the right-hand side of (23) using (24) for m_{0r} . Except for harmonics propagating along the geomagnetic meridian ($k_x = 0$, $k_y \neq 0$) in the narrow vicinity of the magnetic equator ($\sin \gamma \rightarrow 1$), the second term is much smaller than the first. Therefore, it can be neglected compared to the first term. Thus, we arrive at the imaginary part of the vertical wave number $m_i = \epsilon m_{1i}$

$$m_i \approx \frac{v_{\rm ni} m_{0_f}}{2\tilde{\omega}} \frac{k_{\rm x}^2 + k_{\rm y}^2 \cos^2 \gamma}{k_{\rm h}^2},\tag{25}$$

which defines the vertical damping rate acting on the wave amplitude.

4. Implications of the Physical Assumptions

Before proceeding further, we discuss the obtained results along with the used approximations and limitations. Equation (23) shows that, to the first order of $\varepsilon = v_{\rm ni}/\tilde{\omega}$, only the diagonal terms of the matrix (17) (or its equivalent (18) contribute to the wave damping. Among them, damping of the vertical wind is much weaker



than that of the horizontal wind variations and GWs can still be considered hydrostatic for parameterization purposes. The nondiagonal terms containing $v_{\rm ni}$ (and, thus, associated with geomagnetic influence) describe forces acting perpendicular to displacements. These forces are, therefore, conservative in the sense that they do not contribute to GW dissipation. This formalism helps in exploring the consequences of the neglect of the term with the Hall conductivity σ_H in the generalized Ohm's law (6). In addition to σ_H being small compared to σ_ρ in the F region, there is another reason for that. Taking the term ($\sigma_H \mathbf{B}_0 \times \mathbf{v} \times \mathbf{B}_0 \times \mathbf{B}_0$) into account results in additional antisymmetric nondiagonal imaginary terms and zero diagonal part. In other words, effects associated with the Hall conductivity do not contribute to GW dissipation. They describe forces that are directed perpendicular to the components of wave-induced wind fluctuations, similar to the Coriolis force. These forces are important for large-scale and low-frequency waves in the D and E region of the ionosphere (e.g., Kaladze et al., 2007) but are irrelevant for GWs under the midfrequency approximation.

The other exploited assumption was the dipole structure of the geomagnetic field, that is, equating the (geomagnetic) longitudinal component b_x in $\mathbf{b} = (b_x, b_y, b_z)$ to zero. During magnetic storms, however, the dipole can be greatly disturbed, and b_x may no longer be zero. If the parameterization is to be extended for these cases, the term b_x must not be neglected. Given that the off-diagonal terms do not contribute to wave dissipation, it is sufficient to include only the diagonal terms, in particular, in the second row of (17) (see the second equation in (A1). The derivation can be repeated, and the final result will be similar to (25) but with a modified form factor, that is, the ratio containing k_x and k_y .

This form factor describes the dependence of the vertical damping on the azimuth of wave propagation. For harmonics traveling in the zonal direction ($k_y=0$, meridional wind fluctuations v=0), ion friction is independent of latitude (cf. (11). Contrary to that, damping of harmonics propagating in the meridional direction ($k_x=0$, wave disturbances u=0) depends on the magnetic field dip angle γ (cf. (12). Note that the magnitude of the derived vertical damping rate ($v_{\rm ni}m_{\rm 0r}/\bar{\omega}$) coincides with that used in the parameterization of Yiğit et al. (2008, equation (16)), except for the factor 2 that was related to the convention adopted in the latter paper.

We next turn to the consequences of the derived expression for the vertical damping rate (25) by performing calculations with the whole atmosphere GW scheme, which is outlined in the next section.

5. Whole Atmosphere Gravity Wave Scheme

This GW scheme and its development were described in detail in the works of Yiğit et al. (2008) and Yiğit and Medvedev (2013). It has been widely applied in "whole atmosphere" GCMs for Earth (e.g., Yiğit & Medvedev 2010; Yiğit et al., 2016, and references therein) and Mars (e.g., Medvedev et al., 2011, 2013, 2015, 2016; Medvedev & Yiğit, 2012), and has been used to interpret gravity wave observations on Mars (Yiğit et al., 2015). Within the framework of the scheme, the equation for vertical evolution of the horizontal momentum flux (per unit mass) $\overline{u'w'}$ is solved under the midfrequency approximation and relatively small vertical wavelength (m_0 , $H \gg 1$). For a GW harmonic j from a broad spectrum, the equation takes the form

$$\frac{d\overline{u'w'_j}}{dz} = \left(-\frac{\rho_{0z}}{\rho_0} - \beta_{tot}^j\right) \overline{u'w'_j},\tag{26}$$

where primes are reinstated for wave variables, overbars designate averaging over spatial and temporal scales exceeding those of GWs (coarse graining), and the total vertical damping rate represents the sum of damping rates due to all dissipative mechanisms acting on the harmonic in the thermosphere:

$$\beta_{\text{tot}}^{j} = \beta_{\text{non}}^{j} + \beta_{\text{mol}}^{j} + \beta_{\text{rad}}^{j} + \beta_{\text{eddy}}^{j} + \beta_{\text{ion}}^{j} + \text{etc.}$$
 (27)

The damping rates in the right-hand part of (27) are, correspondingly, due to nonlinear breaking/saturation, molecular diffusion and heat conduction, radiative damping, eddy diffusion and heat conduction, and ion drag. After specifying boundary values of $\overline{u'w'}(z_s)$ at a source level z_s in the lower atmosphere, equation (26) is solved upward for individual harmonics in the spectrum, while nonlinear interactions between them are accounted for in β_{non} after the parameterization of Medvedev & Klaassen (1995, 2000). Without dissipation, the wave propagates upward conservatively ($\rho_0 \overline{u'w'} = \text{const}$). A given dissipating harmonic ($\beta_{\text{tot}}^j \neq 0$) deposits its momentum to the mean flow, thus producing the dynamical forcing (wave drag) a_j in the direction of its propagation:

$$a_{j} = -\frac{1}{\rho_{0}} \frac{d(\rho_{0} \overline{u'w'_{j}})}{dz}.$$
 (28)

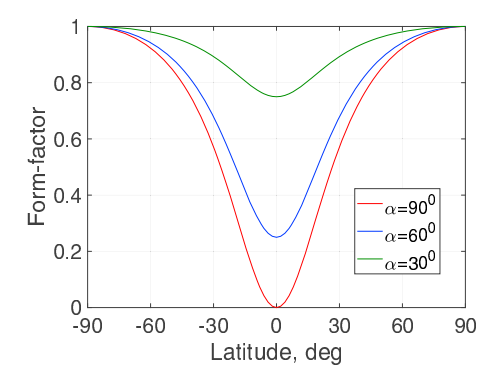


Figure 1. The latitudinal distributions of the form factor $(\cos^2\alpha + \sin^2\alpha\cos^2\gamma)$ from equation (30) for three characteristic propagation azimuths α with respect to the geomagnetic parallel: $\alpha = 90^\circ$ (pure meridional propagation, red), $\alpha = 60^\circ$ (blue) and $\alpha = 30^\circ$ (green). For harmonics propagating zonally ($\alpha = 0^\circ$), the form factor is unity.

Thermal effects of dissipating GWs include heating E_j due to irreversible conversion of mechanical energy into heat, and differential heating/cooling Q_j by inducing a downward sensible heat flux. The expressions for the heating rates (in K s⁻¹) are given after (Medvedev & Klaassen, 2003; Yiğit & Medvedev, 2009)

$$E_{j} = \frac{a_{j}(c_{j} - \bar{u})}{c_{p}}, \qquad Q_{j} = \frac{H}{2\rho_{0}R} \frac{\partial}{\partial z} \left[\rho_{0} a_{j}(c_{j} - \bar{u}) \right], \tag{29}$$

where c_n is the specific heat at constant pressure and R is the gas constant.

6. Results of Calculations

Using the expression for the imaginary part of the vertical wave number (25) and the dispersion relation (24), we can conveniently represent the vertical damping rate due to ion friction in the form

$$\beta_{\text{ion}}^{j} = \frac{v_{\text{ni}}N}{k_{h}|c_{j} - \bar{u}|^{2}} \left(\cos^{2}\alpha + \sin^{2}\alpha\cos^{2}\gamma\right),\tag{30}$$

where α is the azimuth angle (counted counterclockwise from the direction to east) and $\cos^2 \gamma$ is determined by the shape of the geomagnetic field. The

coefficient 2 in the denominator of (25) cancels out, because β_{ion}^l acts on the quadratic with respect to the amplitude quantity. In the first approximation, the geomagnetic field in the F region is a dipole $\mathbf{B} = (0, B_0 \cos \phi, -2B_0 \sin \phi)$, where ϕ is the geomagnetic latitude. Therefore,

$$\cos^2 \gamma \equiv \frac{B_z^2}{|\mathbf{B}|^2} = \frac{4 \sin^2 \phi}{1 + 3 \sin^2 \phi}.$$
 (31)

The expression in the brackets in (30) together with (31) gives the dependence of $\beta_{\rm ion}$ on latitude and propagation azimuth of the harmonic. This "form factor" is illustrated in Figure 1 for harmonics over the equator ($\cos^2 \gamma = 0$) traveling at three characteristic azimuths α : 90° (propagation along the geomagnetic meridian), 60° and 30°. It is seen that damping by ion friction maximizes over the geomagnetic poles (i.e., the form factor of 1) and reduces over the equator. For harmonics traveling in the north-south direction (along the horizontal projection of the geomagnetic dipole), damping by ion friction fully vanishes over the equator. The ion damping acting on harmonics traveling at $\alpha = 60^\circ$ and 30° decreases to ~25% and ~75% of the maximum value over the poles, correspondingly.

How much do these variations of β_{ion} affect vertical propagation and dissipation of GW harmonics as well as the resulting dynamical and thermal effects? To demonstrate this, we present results of calculations with

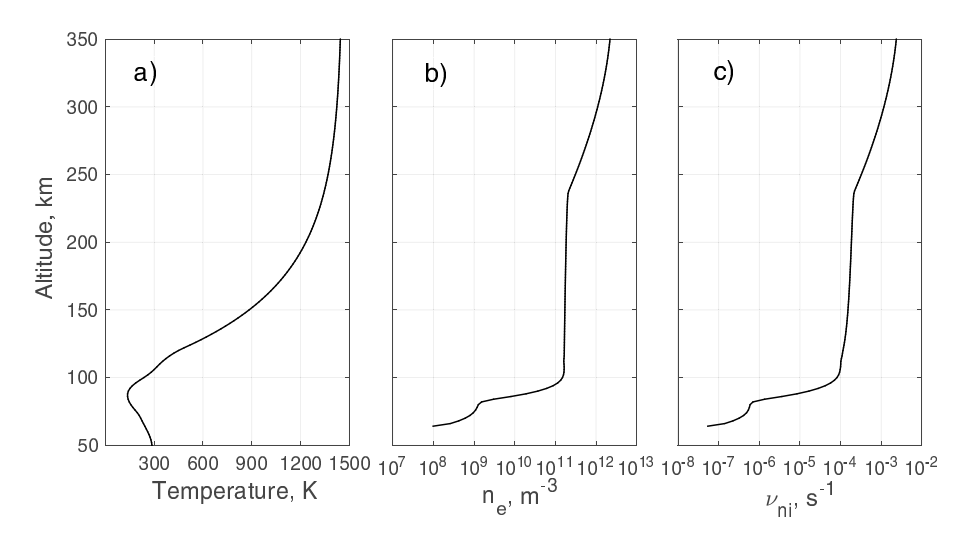


Figure 2. Input profiles used in the calculations: zonally averaged (a) temperature, (b) electron number density n_e from the International Reference Atmosphere (IRI) model, and (c) the calculated neutral-ion collision frequency $v_{\rm ni}$.

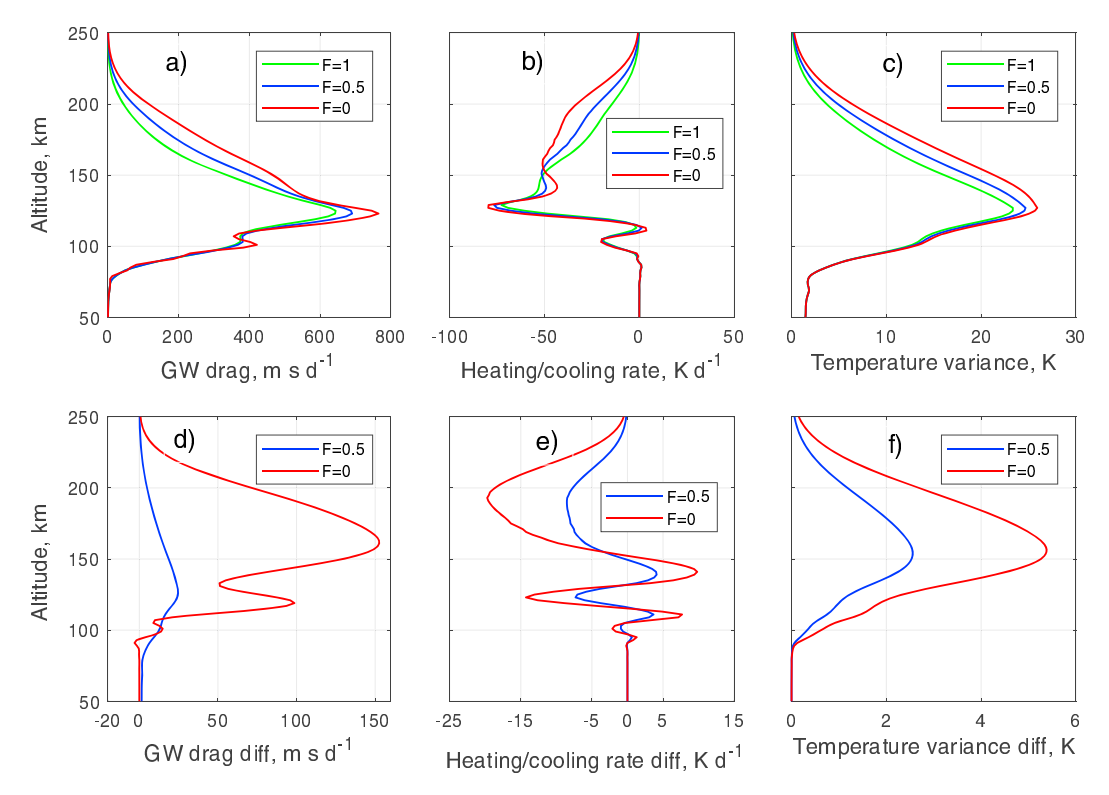


Figure 3. Profiles of the (a) GW drag, (b) cooling/heating rate, and (c) the square root of temperature variance calculated for F = 1 (green), 0.5 (blue), and 0 (red). (d – f) The corresponding differences between the calculations with the reduced ion friction (F = 0.5 and 0) and F = 1.

the GW scheme outlined in the previous section. We used the approximation $v_{\rm ni}=7.22\times10^{-17}T^{0.37}e_i$ (Klostermeyer, 1972) for the neutral-ion collisional frequency $v_{\rm ni}$, where the electron number density e_i and neutral temperature T were taken from the International Reference Ionosphere (IRI) model (Bilitza, 2015) at the equator during an equinox for moderate solar activity conditions ($F_{10.7}=130\times10^{-22}$ W m $^{-2}$ Hz $^{-1}$). Figure 2 presents the vertical profiles of zonally averaged temperature, electron/ion number density corresponding to 31 March and the resulted $v_{\rm nj}$, which served as an input to the column model. Vertical damping by molecular diffusion and thermal conduction cannot be ignored in the thermosphere and was accounted for as described in the work of Yiğit et al. (2008, section 3.3). To avoid the effects of critical level filtering that may mask the influence of damping by ions, calculations have been performed for the windless atmosphere. The GW momentum flux at the lower boundary ($z_{\rm s}=12$ km) was represented by 15 harmonics with the horizontal wavelength 100 km, whose magnitudes were prescribed by the formula $\overline{u'w'}_j=2.6\times10^{-4}$ exp ($-c_j^2/c_w^2$), where phase velocities c_j ranged from 2 to 80 m s $^{-1}$, and the characteristic width of the source spectrum $c_w=35$ m s $^{-1}$ was adopted.

Figure 3 shows profiles of the resulting GW drag (a, d), GW-induced cooling/heating rates (b, e), and temperature variance (c, f) calculated for several characteristic form factors: F = 1, 0.5, and 0. The corresponding differences between the calculations with F = 1 and with reduced ion friction are presented in Figures 3d - 3f. These differences become noticeable above ~ 100 km and grow with height with the increasing ionization. Above 150 km, the GW drag and wave-induced cooling are, respectively, by ~ 150 m s⁻¹ d⁻¹ and ~ 20 K d⁻¹ larger, when ion friction does not affect wave propagation (F = 0). Not only the effects of GWs clearly differ in the upper atmosphere but also the GW variances created by all harmonics in the spectrum. Thus, temperature variance is by ~ 5.5 K larger for the F = 0 case compared to F = 1 (Figure 3f). Such behavior is easily understood, if the components of the vertical damping rate are considered. Figure 4 compares the vertical profiles of $\beta_{\rm ion}$ (dashed lines, calculated assuming F = 1) versus $\beta_{\rm mol}$ for two representative horizontal phase velocities, 5 and 80 m s⁻¹, that is, a slow and a fast wave, respectively. Note that the damping rates are larger for slower harmonics, which explains why faster GWs tend to propagate higher. It is also seen that the effect of ion drag is similar to that of molecular diffusion and heat conduction: faster harmonics experience less

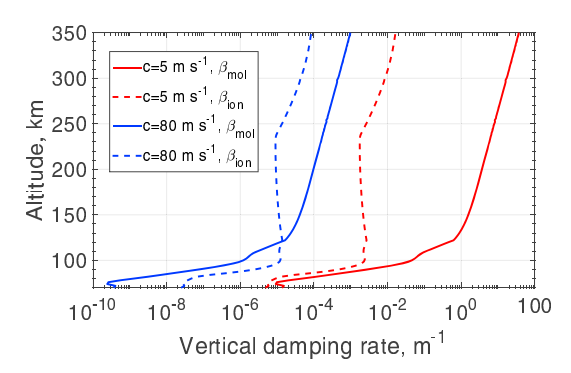


Figure 4. Profiles of vertical damping rates due to molecular diffusion and heat conduction (β_{mol} , solid lines) and due to ion friction (β_{ion}) (dashed lines) for two representative harmonics with the horizontal phase speeds of $c=5~\text{m s}^{-1}$ (red) and 80 m s⁻¹ (blue).

damping and, thus, propagate higher (e.g., Vadas, 2007). The magnitude of $\beta_{\rm ion} \propto m^2/(k_h N) = N/(k_h |c-\bar{u}|^2)$, as follows from (25), whereas $\beta_{\rm mol} \propto m^4/(k_h N) = N^3/(k_h |c-\bar{u}|^4)$ (see Vadas & Fritts, 2005, equations (41) and (47)). Therefore, the ion damping of GWs is less selective (with respect to intrinsic phase velocities or vertical wave numbers) than the viscous one. Figure 4 shows that molecular viscosity and heat conduction are the dominant GW damping mechanism in the thermosphere, exceeding ion friction by several orders of magnitude. Nevertheless, accounting for varying $\beta_{\rm ion}$ results in changes shown in Figure 3, contributing to the variability in a realistic atmosphere. With the lack of ion friction, certain GW harmonics (F=0.5 and 0) can propagate higher, grow in amplitude, and, upon ultimately reaching saturation and obliteration, produce stronger dynamical and thermal forcing on the flow than in the presence of ion friction effect on wave propagation.

7. Summary and Conclusions

The geomagnetic field controls motions of the ionospheric plasma, which, in general, significantly differ from neutral wind dynamics. The mutual interactions of ions and neutrals in the thermosphere-ionosphere (TI) give rise to the ion drag force, which affects gravity wave-induced wind variations. We derived a practical formula for the vertical damping rate of GW harmonics that accounts for the geometry of the magnetic field and arbitrary propagation directions of the waves. This formula (equation (30) together with (31) is suitable for use with parameterizations of GW effects employed in "whole atmosphere" general circulation models (GCMs) extending from the lower atmosphere into the upper thermosphere. For GW harmonics, whose intrinsic frequencies $\tilde{\omega}$ significantly exceed neutral-ion collision frequencies in the F region of the ionosphere, the following results have been obtained:

- 1. In addition to the effect of ion drag (i.e., ion-neutral interactions) on the large-scale circulation in the thermosphere, the anisotropic effect of ion friction on the propagation and dissipation of small-scale GWs has to be taken into account.
- 2. Vertical damping by ion friction depends only on the geometry of the geomagnetic field and does not depend on the strength of the latter.
- 3. Vertical damping by ion friction of GW harmonics propagating in the meridional (in the geomagnetic coordinates) direction varies with latitude, being the strongest over the (magnetic) poles and dropping to zero over the equator. For harmonics propagating in the zonal direction, no latitude dependence for the damping rate exists.
- 4. Estimates from column model calculations using the whole atmosphere GW parameterization of Yiğit et al. (2008) show that taking into account the geometry of the geomagnetic field can, typically, increase GW drag by more than a hundred m s⁻¹ d⁻¹, GW cooling/heating rate by \sim 15 K d⁻¹, and GW-induced temperature variance by several K at *F* region heights.

GWs arriving to the upper thermosphere from below undergo a strong filtering by mean winds in the underlying layers. The anisotropy (i.e., directional dependence) of GW damping by ion friction in combination with selective filtering of harmonics can significantly modify the established picture of GW-mean flow interactions in the upper thermosphere and provide a new perspective to wave-induced variability in the TI. More realistically, these effects and consequences for the troposphere-thermosphere-ionosphere coupling can be explored with GCMs.

Appendix A

In order to assist in reproducing the derivations in sections 2 and 3, and discussion in section 4, we present here the expressions for some cross products. For the wave-induced wind disturbances $\mathbf{v} = (u, v, w)$ and the unit geomagnetic vector $\mathbf{b} = (b_x, b_y, b_z) \equiv \mathbf{B}/B$, where B is the absolute value of \mathbf{B} :

$$\mathbf{v} \times \mathbf{b} = \begin{pmatrix} b_z v - b_y w \\ -b_z u + b_x v \\ b_y u - b_x v \end{pmatrix}, \qquad \mathbf{v} \times \mathbf{b} \times \mathbf{b} = \begin{pmatrix} -(b_y^2 + b_z^2)u + (b_x b_y + b_x b_z)v \\ b_x b_y u - (b_x^2 + b_z^2)v + b_y b_z w \\ b_x b_z u + (b_y b_z - b_x^2)v - b_y^2 w \end{pmatrix}, \tag{A1}$$



The derivation of the last equality in (10) can be performed directly without resorting to the components of the cross products. Thus,

$$\mathbf{v}' \times \mathbf{B}_0 \times \mathbf{B}_0 = -\mathbf{B}_0 \times (\mathbf{v}' \times \mathbf{B}_0) = -[\mathbf{v}'B^2 - (\mathbf{v}' \cdot \mathbf{B}_0)\mathbf{B}_0], \tag{A2}$$

and note (9) for the expression for σ_n .

Acknowledgments

The modeling data supporting the figures presented in this paper can be obtained at https://zenodo.org/record/ 1045415#.Waca5Wdc5d4 (doi:10.5281/zenodo.1045415). This work was partially supported by German Science Foundation (DFG) grant HA3261/8-1, which is the part of the DFG priority program SPP1788 "Dynamic Earth". E. Y. was partially funded by the National Science Foundation (NSF) grant AGS 1452137.

References

- Artru, J., Ducic, V., Kanamori, H., Lognonne, P., & Murakami, M. (2005). Ionospheric detection of gravity waves induced by tsunamis. Geophysical Journal International, 160, 840-848. https://doi.org/10.1111/j.1365-246X. 2005.02552.x
- Bilitza, D. (2015). The international reference ionosphere—Status 2013. Advances in Space Research, 55, 1914-1927. https://doi.org/10.106/j.asr.2014.07.032
- de la Torre, A., Alexander, P., Llamedo, P., Hierro, R., Nava, B., Radicella, S., ... Wickert, J. (2014). Wave activity at ionospheric heights above the Andes Mountain as detected from FORMOSAT-3/COSMIC GPS radio occultation data. Journal of Geophysical Research: Space Physics, 119, 2046-2051. https://doi.org/10.1002/2013JA018870
- Forbes, M. F., Bruinsma, S. L., Doornbas, E., & Zhang, X. (2016). Gravity wave-induced variability of the middle thermosphere. Journal of Geophysical Research: Space Physics, 121, 6914-6923. https://doi.org/10.1002/2016JA022923
- Francis, S. H. (1973). Acoustic-gravity modes and large-scale traveling ionospheric disturbances of a realistic, dissipative atmosphere. Journal of Geophysical Research, 78, 2278–2301.
- Fritts, D. C., & Alexander, M. J. (2003). Gravity wave dynamics and effects in the middle atmosphere. Reviews of Geophysics, 41(1), 1003. https://doi.org/10.1029/2001RG000106
- Fritts, D. C., & Lund, T. S. (2011). Gravity wave influences in the thermosphere and ionosphere: Observations and recent modeling. In Aeronomy of the Earth's Atmosphere and Ionosphere (pp. 109–130). Dordrecht, Netherlands: Springer.
- Garcia, R. F., Doornbos, E., Bruinsma, S., & Hebert, H. (2014). Atmospheric gravity waves due to the Tohoku-Oki tsunami observed in the thermosphere by GOCE. Journal of Geophysical Research; Atmospheres, 119, 4498-4506. https://doi.org/10.1002/2013JD021120
- Gavrilov, N. M., & Kshevetskii, S. P. (2013). Numerical modeling of propagation of breaking nonlinear acoustic-gravity waves from the lower to the upper atmosphere. Advances in Space Research, 51, 1168-1174. https://doi.org/10.1016/j.asr.2012.10.023
- Goncharenko, L. P., Hsu, V. W., Brum, C. G. M., Zhang, S.-R., & Fentzke, J. T. (2013). Wave signatures in the midlatitude ionosphere during a sudden stratospheric warming of January 2010. Journal of Geophysical Research: Space Physics, 118, 472-487. https://doi.org/10.1029/2012JA018251
- Heale, C. J., Snively, J. B., Hickey, M. P., & Ali, C. J. (2014). Thermospheric dissipation of upward propagating gravity wave packets. Journal of Geophysical Research: Space Physics, 119, 3857-3872. https://doi.org/10.1002/2013JA019387
- Hickey, M. P., & Cole, K. D. (1987). A quartic dispersion equation for internal gravity waves in the thermosphere. Journal of Atmospheric and Solar-Terrestrial Physics, 49, 889 - 899.
- Hickey, M. P. (2011). Atmospheric gravity waves and effects in the upper atmosphere associated with tsunamis (InTech): The Tsunami Threat-Research and Technology. https://doi.org/10.5772/13577. Retrieved from https://www.intechopen.com/books/the-tsunamithreat-research- and -technology/atmospheric-gravity-waves- and -effects-in-the-upper-atmosphere- associated-with-ts unamisation of the second of the seco
- Hines, C. O. (1955). Hydromagnetic resonance in jonospheric waves, Journal of Atmospheric and Solar-Terrestrial Physics, 7, 14 30.
- Hines, C. O., & Hooke, W. H. (1970). Discussion of ionization effects on the propagation of acoustic-gravity waves in the ionosphere. Journal of Geophysical Research, 75, 2563 - 2568.
- Hocke, K., & Schlegel, K. (1996). A review of atmospheric gravity waves and travelling ionospheric disturbances: 1982 1995. Annales de Geophysique, 14, 917-940.
- Hung, R. J., Phan, T., & Smith, R. E. (1979). Coupling of ionosphere and troposphere during the occurrence of isolated tornadoes on November 20, 1973. Journal of Geophysical Research, 84, 1261 – 1268. https://doi.org/10.1029/JA084A04p01261
- Kaladze, T. D., Pokhotelov, O. A., Stenflo, L., Shah, H. A., & Jandieri, G. V. (2007). Electromagnetic inertio-gravity waves in the ionospheric E-layer. Physica Scripta, 76, 343-348. https://doi.org/10.1088/0031-8949/76/4/011
- Kelley, M. C. (2009). The Earth's ionosphere: Plasma physics and electrodynamics, International Geophysics (Vol. 96): Amsterdam: Elsevier Science.
- Kirchengast, G. (1997). Characteristics of high-latitude TIDs from different causative mechanisms deduced by theoretical modeling. Journal of Geophysical Research, 102, 4597-4612.
- Klostermeyer, J. (1972). Influence of viscosity, thermal conduction, and ion drag on the propagation of atmospheric gravity waves in the thermosphere. Zeitschrift für Geophysik, 38, 881 – 890.
- Liu, C. H., & Yeh, K. C. (1969). Effect of ion drag of acoustic-gravity waves in the atmospheric F region. Journal of Geophysical Research, 74,
- Liu, H., Jin, H., Miyoshi, Y., Fujiwara, H., & Shinagawa, H. (2013). Upper atmosphere response to stratosphere sudden warming: Local time and height dependence simulated by GAIA model. Geophysical Research Letters, 40, 635-640. https://doi.org/10.1002/grl.50146
- Medvedev, A. S., & Klaassen, G. P. (1995). Vertical evolution of gravity wave spectra and the parameterization of associated wave drag. Journal of Geophysical Research, 100, 25841-25853.
- Medvedev, A. S., & Klaassen, G. P. (2000). Parameterization of gravity wave momentum deposition based on nonlinear wave interactions: Basic formulation and sensitivity tests. Journal of Atmospheric and Solar-Terrestrial Physics, 62, 1015 – 1033.
- Medvedev, A. S., & Klaassen, G. P. (2003). Thermal effects of saturating gravity waves in the atmosphere. Journal of Geophysical Research, 108, 4040. https://doi.org/10.1029/2002JD002504
- Medvedev, A. S., Yiğit, E., Hartogh, P., & Becker, E. (2011). Influence of gravity waves on the Martian atmosphere: General circulation modeling. Journal of Geophysical Research, 116, E10004. https://doi.org/10.1029/2011JE003848
- Medvedev, A. S., Yiğit, E., Kuroda, T., & Hartogh, P. (2013). General circulation modeling of the Martian upper atmosphere during global dust storm. Journal of Geophysical Research, 118, 2234-2246. https://doi.org/10.1002/2013JE004429
- Medvedev, A. S., González-Galindo, F., Yiğit, E., Feofilov, A. G., Forget, F., & Hartogh, P. (2015). Cooling of the Martian thermosphere by CO₂ radiation and gravity waves: An intercomparison study with two general circulation models. Journal of Geophysical Research: Planets, 120, 913-927. https://doi.org/10.1002/2015JE004802
- Medvedev, A. S., Nakagawa, H., Mockel, C., Yiğit, E., Kuroda, T., Hartogh, P., . . . Jakosky, B. M. (2016). Comparison of the Martian thermospheric density and temperature from IUVS/MAVEN data and general circulation modeling. Geophysical Research Letters, 43, 3095 - 3104. https://doi.org/10.1002/2016GL068388

DAGU Journal of Geophysical Research: Space Physics

- Medvedev, A. S., & Yiğit, E. (2012). Thermal effects of internal gravity waves in the Martian thermosphere. Geophysical Research Letters, 39, L05201. https://doi.org/10.1029/2012GL050852
- Miesen, R. H. M., de Jagher, P. C., Kamp, L. P. J., & Sluuter, F. W. (1989). Damping of acoustic gravity waves caused by the conductivity of the ionosphere. Journal Geophysical Research, 94, 16,269 - 15,275.
- Miesen, R. H. M. (1991). Damping rates for acoustic gravity waves in the ionosphere. Journal Geophysical Research, 96, 15,359 15,364. Miller, S. D., Straka, W. C., Yue, J., Smith, S. M., Alexander, M. J., Hoffmann, L., ... Partain, P. T. (2015). Upper atmospheric gravity wave details revealed in nightglow satellite imagery. Proceedings of the National Academy of Sciences USA, 112, E6728-E6735. https://doi.org/10.1073/pnas.1508084112
- Miyoshi, Y., Fujiwara, H., Jin, H., & Shinagawa, H. (2014). A global view of gravity waves in the thermosphere simulated by a general circulation model. Journal of Geophysical Research: Space Physics, 119, 5807-5820. https://doi.org/10.1002/2014JA019848
- Munro, G. H. (1950). Travelling disturbances in the ionosphere. Proceedings Royal Society of London, 202, 208-223. https://doi.org/10.1098/rspa.1950.0095
- Pogoreltsev, A. I. (1996). Production of electromagnetic field disturbances due to interaction between acoustic gravity waves and the ionospheric plasma, Journal of Atmospheric and Solar-Terrestrial Physics, 59, 1391 – 1403,
- Vadas, S. L. (2007). Horizontal and vertical propagation and dissipation of gravity waves in the thermosphere from lower atmospheric and thermospheric sources. Journal of Geophysical Research, 112, A06305. https://doi.org/10.1029/2006JA011845
- Vadas, S. L., & Crowley, G. (2010). Sources of the traveling ionospheric disturbances observed by the ionospheric TIDDBIT sounder near Wallops Island on 30 October 2007. Journal of Geophysical Research, 115, A07324. https://doi.org/10.1029/2009JA015053
- Vadas, S. L., & Fritts, D. C. (2005). Thermospheric responses to gravity waves: Influences of increasing viscosity and thermal diffusivity. Journal of Geophysical Research, 110, D15103. https://doi.org/10.1029/2004JD005574
- Vasyliūnas, V. M. (2012). The physical basis of ionospheric electrodynamics. Annales de Geophysique, 30, 357-369. https://doi.org/10.5194/angeo-30-357-2012
- Yiğit, E. (2017). Atmospheric and space sciences: Ionospheres and plasma environments, SpringerBriefs in Earth Science (Vol. 2). Netherlands: Springer. https://doi.org/10.1007/978-3-319-62006-0
- Yiğit, E., & Medvedev, A. S. (2009). Heating and cooling of the thermosphere by internal gravity waves. Journal of Geophysical Letters, 36, L14807. https://doi.org/10.1029/2009GL038507
- Yiğit, E., & Medvedev, A. S. (2010). Internal gravity waves in the thermosphere during low and high solar activity: Simulation study. Journal of Geophysical Research, 115, A00G02. https://doi.org/10.1029/2009JA015106
- Yiğit, E., & Medvedev, A. S. (2012). Gravity waves in the thermosphere during a sudden stratospheric warming. Journal of Geophysical Letters, 39, L21101. https://doi.org/10.1029/2012GL053812
- Yiğit, E., & Medvedev, A. S. (2013). Extending the parameterization of gravity waves into the thermosphere and modeling their effects. In Lübken, F.-J. (Ed.), Climate and Weather of the Sun-Earth System (CAWSES), Springer Atmospheric Sciences (pp. 467–480). Dordrecht, Netherlands: Springer. https://doi.org/10.1007/978-94-007-4348-9_25
- Yiğit, E., & Medvedev, A. S. (2015). Internal wave coupling processes in Earth's atmosphere. Advances in Space Research, 55, 983 1003. https://doi.org/10.1016/j.asr.2014.11.020
- Yiğit, E., & Medvedev, A. S. (2016). Role of gravity waves in vertical coupling during sudden stratospheric warmings. Geoscience Letters, 3, 27. https://doi.org/10.1186/s40562-016-0056-1
- Yiğit, E., & Medvedev, A. S. (2017). Influence of parameterized small-scale gravity waves on the migrating diurnal tide in Earth's thermosphere. Journal of Geophysical Research: Space Physics, 122, 4846–4864. https://doi.org/10.1002/2017JA024089
- Yiğit, E., Aylward, A. D., & Medvedev, A. S. (2008). Parameterization of the effects of vertically propagating gravity waves for thermosphere general circulation models: Sensitivity study. Journal of Geophysical Research, 113, D19106. https://doi.org/10.1029/2008JD010135
- Yiğit, E., Medvedev, A. S., Aylward, A. D., Hartogh, P., & Harris, M. J. (2009). Modeling the effects of gravity wave momentum deposition on the general circulation above the turbopause. Journal of Geophysical Research, 114, D07101. https://doi.org/10.1029/2008JD011132
- Yiğit, E., Medvedev, A. S., Aylward, A. D., Ridley, A. J., Harris, M. J., Moldwin, M. B., & Hartogh, P. (2012). Dynamical effects of internal gravity waves in the equinoctial thermosphere. Journal of Atmospheric and Solar-Terrestrial Physics, 90-91, 104-116. https://doi.org/10.1016/j.jastp.2011.11.014
- Yiğit, E., Medvedev, A. S., England, S. L., & Immel, T. J. (2014). Simulated variability of the high-latitude thermosphere induced by small-scale gravity waves during a sudden stratospheric warming. Journal of Geophysical Research: Space Physics, 119, 357-365. https://doi.org/10.1002/2013JA019283
- Yiğit, E, England, S. L., Liu, G., Medvedev, A. S., Mahaffy, P. R., Kuroda, T., & Jakosky, B. (2015). High-altitude gravity waves in the Martian thermosphere observed by MAVEN/NGIMS and modeled by a gravity wave scheme. Geophysical Research Letters, 42, 8993 – 9000. https://doi.org/10.1002/2015GL065307
- Yiğit, E., Knížová, P. K., Georgieva, K., & Ward, W. (2016). A review of vertical coupling in the atmosphere-ionosphere system: Effects of waves, sudden stratospheric warmings, space weather, and of solar activity. Journal of Atmospheric and Solar-Terrestrial Physics, 141, 1–12. https://doi.org/10.1016/j.jastp.2016.02.011